Developmental and Comparative Immunology 156 (2024) 105170

Contents lists available at ScienceDirect

Developmental and Comparative Immunology

journal homepage: www.elsevier.com/locate/devcompimm

USP46 promotes the interferon antiviral signaling in black carp by deubiquitinating TBK1

Juanjuan Shu [a,1], Can Yang [a,1], Yujia Miao [a], Jinyi Li [a], Tianle Zheng [a], Jun Xiao [a,*], Weiguang Kong [b], Zhen Xu [b], Hao Feng [a,**]

[a] State Key Laboratory of Developmental Biology of Freshwater Fish, College of Life Science, Hunan Normal University, Changsha, China
[b] State Key Laboratory of Freshwater Ecology and Biotechnology, Institute of Hydrobiology, Chinese Academy of Sciences, Wuhan, China

ARTICLE INFO

Keywords:
USP46
TBK1
Interferon
Deubiquitination
Black carp

ABSTRACT

Ubiquitin-specific peptidase 46 (USP46) functions as a deubiquitinating enzyme, facilitating the removal of ubiquitin molecules attached to substrate proteins and playing a critical role in cancer and neurodegenerative diseases. However, its function in innate antiviral immunity is unknown. In this study we cloned and identified bcUSP46, a homolog of USP46 from black carp. We discovered that overexpression of bcUSP46 enhanced the transcription of interferon (IFN) promoters and increased the expression of *IFN*, *PKR*, and *Mx1*. In addition, bcUSP46 knockdown significantly inhibited the expression of ISG genes, as well as the antiviral activity of the host cells. Interestingly, when bcUSP46 was co-expressed with the RLR factors, it significantly enhanced the activity of the IFN promoter mediated by these factors, especially TANK-binding kinase 1 (TBK1). The subsequent co-immunoprecipitation (co-IP) and immunofluorescence (IF) assay confirmed the association between bcUSP46 and bcTBK1. Noteworthily, co-expression of bcUSP46 with bcTBK1 led to an elevation of bcTBK1 protein level. Further analysis revealed that bcUSP46 stabilized bcTBK1 by eliminating the K48-linked ubiquitination of bcTBK1. Overall, our findings highlight the unique role of USP46 in modulating TBK1/IFN signaling and enrich our knowledge of the function of deubiquitination in regulating innate immunity in vertebrates.

1. Introduction

For defense against viral infection, vertebrates have robust immune systems that include innate immunity and adaptive immunity. The former has been conserved throughout evolution, acts as the initial line of defense against viral invasion. Upon viral infection, pattern recognition receptors (PRRs) in the host cells recognize the presence of pathogen-associated molecular patterns (PAMPs). This triggers the recruitment of the downstream adaptors and initiates strings of downstream cascades to establish an antiviral state in host cells (Cao, 2016). In this process, TBK1 is a key regulator of cellular antiviral signaling, which could phosphorylate and activate downstream transcription factors including IRFs and NF-κB. Finally, the expression of interferons or inflammatory cytokines was activated (Fitzgerald et al., 2003; Runde et al., 2022).

As an essential kinase in the innate immune response, TBK1 activity can be regulated by ubiquitination. Studies have demonstrated that E3 ligases MIB and Nrdp1 are responsible for modulating the K63 ubiquitination of TBK1 in its reaction to RNA viruses and LPS, respectively (Li et al., 2011; Wang et al., 2009), but the effect of deubiquitinating enzymes (DUB) on TBK1 activity remains unclear. The human genome encodes about 100 deubiquitinating enzymes, which can be classified into metalloproteases and cysteine proteases according to their different catalytic mechanisms (Komander et al., 2009). Metalloproteases belong only to the JAMM family, and STAM-binding protein (STAMBP) belongs to the JAMM metalloprotease subfamily. In Triple-negative breast cancer (TNBC), STAMBP can stabilize RAI14 protein by inhibiting the ubiquitination of the RAI14-K48 link, thus preventing its proteasomal degradation and thus becoming a potential target for therapy (Yang et al., 2022). It has been shown that cysteine proteases can be further classified into six families based on their sequence conservation and structural domain structure, of which ubiquitin-specific proteases (USP)

* Corresponding author.
** Corresponding author.
E-mail addresses: xiaojun2018@hunnu.edu.cn (J. Xiao), fenghao@hunnu.edu.cn (H. Feng).
[1] These authors contributed equally to this paper.

https://doi.org/10.1016/j.dci.2024.105170
Received 26 December 2023; Received in revised form 23 February 2024; Accepted 22 March 2024
Available online 22 March 2024

Table 1
Plasmids used in this study.

Plasmid	Application
Overexpression	
pcDNA5/FRT/TO-Flag-bcUSP46	Immunoblotting
pcDNA5/FRT/TO-Myc-bcUSP46	Immunofluorescence Microscopy
pcDNA5/FRT/TO-HA-bcTBK1	Luciferase report assay
pcDNA5/FRT/TO-EGFP-bcTBK1	qRT-PCR
pcDNA5/FRT/TO-Flag-bcRIG-Ib	
pcDNA5/FRT/TO-Flag-bcMAVS	
pcDNA5/FRT/TO-Flag-bcIRF3	
pcDNA5/FRT/TO-Flag-bcIRF7	
pcDNA5/FRT/TO-HA-Ub	
pcDNA5/FRT/TO-HA-K48O	
Luciferase Reporter Assay	
Luci-bcIFNa	Black Carp IFNa and EPC IFN Promoter Activity Analysis
Luci-epcIFN	
pRL-TK	
Knock-Down	
pLKO.1-sh-scramble	Knock-Down bcUSP46 in MPK cells
pLKO.1-sh-bcUSP46-1	
pLKO.1-sh-bcUSP46-2	
pLKO.1-sh-bcUSP46-3	

are the largest family with 58 members. Structural analysis of the proteins reveals that the members of this family are structurally "hand-like", consisting of the thumb, palm, and fingers.

The USP46 belongs to the cysteine proteases that deubiquitinate a variety of substrates (Hodul et al., 2017). This protein possesses a ubiquitin carboxy-terminal hydrolase (UCH) domain (Yin et al., 2015). Studies have shown that Xenopus development is associated with USP46 affecting its histone ubiquitination (Joo et al., 2011). In recent years, its function in cancers has garnered significant attention. Many studies have shown that USP46 is a tumor suppressor in colon, renal cell, liver, and lung cancers (Fitzgerald et al., 2003). Conversely, other studies have reported that the deubiquitinating activity of USP46 promotes the growth of tumors by preserving the stability of Cdt2 and ENO1 (Kiran et al., 2018; Tian et al., 2020). Nevertheless, it is obscure how USP46 functions in the antiviral immune responses.

In the present study, the USP46 counterpart from black carp (bcUSP46) was identified. Our results revealed that the antiviral innate immune responses are positively regulated by bcUSP46. Mechanistically, bcUSP46 targets bcTBK1 to remove its K48-linked polyubiquitination, thereby stabilizing bcTBK1 and promoting interferon production. Thus, our study reveals a novel role of USP46 in TBK1/IFN signaling and extends to the comprehension of the function of deubiquitination in innate antiviral responses in vertebrates.

2. Materials and methods

2.1. Cells and plasmids

HEK-293T cells, EPC cells, and *Mylopharyngodon piceus* kidney (MPK) were kept in our laboratory. HEK-293T cells were cultured at 37 °C with 5% CO_2; EPC and MPK cells were cultured at 26 °C with 5% CO_2. All cell lines were maintained in the Dulbecco's Modified EagleMedium (DMEM) (Yuanpei, China) containing 10% fetal bovine serum (FBS), 2 mM glutamine, 100 U/ml penicillin and 100 μg/ml streptomycin. Plasmids were shown in Table 1. All the primer sequences were referenced in Table 2.

2.2. Protein sequence, structure, and phylogenetic analysis

Protein sequences of homologs of USP46 were acquired from the NCBI database. Multiple sequence comparison was conducted using GENEDOC and MEGA6 software. The phylogenetic tree was embellished using i-TOL. The genomic of bcUSP46 was retrieved from the black carp genome database in our lab. The predicted structures of bcUSP46 and human USP46 were generated using Swiss-model and PyMOL.

2.3. qRT-PCR assay

Total RNA was extracted using the RNA rapid extraction kit (Magen, China). The RNA was reverse-transcribed using reverse transcriptase (Takara, Japan). Relative mRNA levels were detected by quantitative real-time PCR (qRT-PCR) using SYBR Green. The PCR programs were as follows: 1 cycle of 95 °C for 10 min, followed by 42 cycles of 95 °C for 15 s, 60 °C for 1 min. The relative mRNA change was calculated by comparison with the corresponding control group using the $2^{-\triangle\triangle CT}$ (where CT is the threshold period) method.

2.4. Luciferase reporter assay

EPC cells were cultured overnight in 24-well plates. EPC cells in 24-well plates were co-transfected with described plasmids together with pRL-TK and different fish IFN promoters (bcIFNa-pro or EPC–IFN–pro). The total amount of plasmids for each transfection was balanced with empty vectors, pcDNA5/FRT/TO. Cells were washed with PBS 24 h after transfection and lysed with passive lysis buffer (PLB) for 15 min, and then assayed for luciferase activity according to the instructions of the Dual Luciferase Reporter Assay System Kit (Promega, USA).

2.5. Immunofluorescence microscopy

EPC cells were transfected with the indicated plasmids for 24 h. The cells were fixed with 4% paraformaldehyde for 15 min, permeabilized with Triton X-100 (0.2% in PBS) for 15 min, and blocked with 10% goat serum (solarbio SL038). Then the cells were incubated with the anti-Flag antibody (Abmart, M20008) or anti-HA antibody (Abmart, M20003) for 1 h. After being washed three times with PBS, the cells were incubated with the corresponding secondary antibody including Alexa 594 (Thermo, 35511) and Alexa 488 (Thermo, 35553). Then 5 μl DAPI (Sigma, USA) was added to the microslide for nuclear staining. Finally, the cells were scanned under a confocal microscope (Olympus).

2.6. Co-IP assay

For the co-IP assays, HEK-293T cells were seeded into 10-cm cell dishes overnight and then transfected with the indicated plasmids. At 48 h post-transfection (hpt), the cells were washed with PBS twice and lysed in 1 ml of lysis buffer. The cellular debris was removed by centrifugation at 12,000×*g* for 5 min at 4 °C. Then supernatant was collected as the whole cell lysate (WCL), while another cell supernatant was added to protein A/G agarose beads and placed on a turntable at 4 °C for 2 h to remove non-specific binding proteins. Two hours later, the protein A/G agarose beads were sedimented by centrifugation at 5000×*g* for 1 min at 4 °C. The cell supernatant was then incubated with Flag beads (Sigma, A2220) and incubated overnight at 4 °C. The immunoprecipitated proteins were collected by centrifugation at

Table 2
Primers used in the study.

Primer name	Sequence (5′-3′)	Primer information
CDS		
bcUSP46-F1	ATGACTGTCAGAAACATCGCC	For bcUSP46
bcUSP46-R1	CTAGAGATTTTCTCTGGACTG	CDS cloning
Expression vector		
bcUSP46-F	ACTGACGGTACCATGACTGTCAGAAACAT	For expression vector construction
bcUSP46-R	ACTGACCTCGAGCTAGAGATTTTCTCTGG	
qRT-PCR		
q-bcUSP46-F	AAACAAGAGGCACAGAAACG	For qRT-PCR assays
q-bcUSP46-R	GTGAACCACCACAGCGACAA	
q-SVCV-*M*-F	CGACCGCGCCAGTATTGATGGATAC	
q-SVCV-*M*-R	ACAAGGCCGACCCGTCAACAGAG	
q-SVCV-N-F	GGGTCTTTACAGAGTGGG	
q-SVCV-N-R	TTTGTGAGTTGCCGTTAC	
q-SVCV-P-F	AACAGGTATCGACTATGGAAGAGC	
q-SVCV-P-R	GATTCCTCTTCCCAATTGACTGTC	
q-SVCV-G-F	GATGACTGGGAGTTAGATGGC	
q-SVCV-G-R	ATGAGGGATAATATCGGCTTG	
q-EPC Viperin-F	ATGAAAACTCAAATGTGGACGTA	
q-EPC Viperin-R	GATAGTTTCCACCCATTTCCTTAA	
q-EPC PKR-F	ACCTGAAGCCTCCAAACATA	
q-EPC PKR-R	GCATTCGCTCATCATTGTC	
q-EPC Mx1-F	TGGAGGAACCTGCCTTAAATAC	
q-EPC Mx1-R	GTCTTTGCTGTTGTCAGAAGATTAG	
q-EPC actin-F	AAGGAGAAGCTCTGCTATGTGGCT	
q-EPC actin-R	AAGGTGGTCTCATGGATACCGCAA	
q-EPC IFN-F	ATGAAAACTCAAATGTGGACGTA	
q-EPC IFN-R	GATAGTTTCCACCCATTTCCTTAA	
q-bc IFNa–F	AAGGTGGAGGACCAGGTGAAGTTT	
q-bc IFNa-R	GACTCCTTATGTGATGGCTTGTGG	
q-bc Mx1-F	TGAGCGTAGGCATTAGCAC	
q-bc Mx1-R	CCTGGAGCAGCAGATAGCG	
q-bc Viperin-F	CCAAAGAGCAGAAAGAGGGACC	
q-bc Viperin-R	TCAATAGGCAAGACGAACGAGG	
q-bc actin-F	TGGGCACCGCTGCTTCCT	
q-bc actin-R	TGTCCGTCAGGCAGCTCAT	
shRNA		
bcUSP46-shRNA-1-F	CCGGGGAAGGAGAATGACCTGTTTGCTCGAGCAAACAGGTCATTCTCCTTCCTTTTTG	plKO.1-shbcUSP46
bcUSP46-shRNA-1-R	AATTCAAAAGGAAGGAGAATGACCTGTTTGCTCGAGCAAACAGGTCATTCTCCTTCC	construction
bcUSP46-shRNA-2-F	CCGGGCCCACCTGGGTTCATGATATCTCGAGATATCATGAACCCAGGTGGGCTTTTTG	
bcUSP46-shRNA-2-R	AATTCAAAAGCCCACCTGGGTTCATGATATCTCGAGATATCATGAACCCAGGTGGGC	
bcUSP46-shRNA-3-F	CCGGGCTGCATCGGTACACTAAACTCTCGAGAGTTTAGTGTACCGATGCAGCTTTTTG	
bcUSP46-shRNA-3-R	AATTCAAAAGCTGCATCGGTACACTAAACTCTCGAGAGTTTAGTGTACCGATGCAGC	

5000×*g* for 1 min at 4 °C, washed three times with lysis buffer, and resuspended in 5 × SDS loading buffer. The immunoprecipitates and whole cell lysates were subjected to Western blotting.

2.7. Western blotting

Cell samples were mixed with 5 × SDS loading buffer and separated on SDS-polyacrylamide gels at appropriate concentrations. Subsequently, the proteins were transferred to polyvinylidene fluoride (PVDF) membranes (Millipore, USA). The PVDF membranes were blocked with skim milk for 1h, followed by further incubation of the primary antibody overnight at 4 °C. After washing the membranes three times with TBS and once with TBST, they were incubated with the secondary antibody for 1 h. Finally, the target proteins were visualized by BCIP/NBT Alkaline Phosphatase Color Development Kit (Sigma, USA).

2.8. Virus production and titer detection

Spring viremia of carp virus (strain: SVCV741) was kept in the lab and propagated in EPC independently in the presence of 2% FBS at 26 °C. Viral titers were assessed by plaque assay in EPC cells. Briefly, viruses were serially diluted 10-fold and the diluted virus arrays were added to EPC cells. After incubation for 1 h, the medium was replaced with fresh DMEM containing 2% FBS and 0.75% methylcellulose (Sigma, USA). At 3 days post-infection, the plaques were measured. We chose the wells that generated the plaque number under 20 and counted. The plaque numbers were multiplied by the dilution ratio (10^1–10^4, etc.) and being manipulated through the normalized process then presented as the titer of SVCV Log10 (PFU/mL).

2.9. Knockdown assay

The shRNA oligos were designed based on the nucleotide sequence of bcUSP46 using a shRNA library from Sigma. Primers were added to ddH_2O and diluted to 20 μM according to the primer annotation. 5 μl of each oligonucleotide, 25 μl of 10 × NEB buffer, and 5 μl of ddH_2O were added to the PCR tubes according to the annealing system, and annealed for 5 min in a 95 °C water bath before being brought to room temperature. Double cleavage of 1 μg of PLKO.1 vector was performed with restriction endonucleases *Eco*R I and *Age*I. Ligation of primers to vectors, purification, and sequencing.

2.10. Statistics analysis

The qRT-PCR, luciferase reporter assay, and virus titration assay were expressed as the mean ± SEM. Data are representative of three independent experiments. Statistical analysis was performed by two-way analysis of variance (ANOVA), Tukey, and Student's t-test using GraphPad Prism 8.0 (GraphPad Software). *$P < 0.05$, **$P < 0.01$.

Table 3
Comparison of bcUSP46 with other vertebrate USP46 (%).

Species	Accession No.	Similarity	Identity
Mylopharyngodon piceus	OR224866	100	100
Megalobrama amblycephala	XP_048062643.1	99.5	99.5
Labeo rohita	XP_050995142.1	99.4	99.2
Puntigrus tetrazona	XP_043076293.1	99.4	98.9
Cyprinus carpio	XP_042611806.1	99.2	98.9
Myxocyprinus asiaticus	XP_051581261.1	99.2	98.6
Danio rerio	NP_001231910.1	99.2	98.1
Carassius gibelio	XP_052390649.1	98.6	98.4
Triplophysa rosa	KAI7800261.1	99.4	98.6
Pimephales promelas	XP_039548971.1	98.6	98.6
Xyrauchen texanus	XP_051953868.1	98.4	98.1
Periophthalmus magnuspinnatus	XP_033821394.1	98.7	97.3
Labrus bergylta	XP_020499432.1	97.8	97.3
Cheilinus undulatus	XP_041647971.1	98.4	97.8
Xiphias gladius	XP_039985230.1	98.4	97.8
Salarias fasciatus	XP_029939327.1	98.4	97.6
Salmo salar	XP_014024451.1	97.6	96.8
Mauremys reevesii	XP_039397474.1	95.8	94.4
Terrapene carolina triunguis	XP_024071948.1	95.8	94.4
Mus musculus	NP_808229.1	95.9	94.6
Perognathus longimembris pacificus	XP_048219870.1	95.9	94.3
Falco cherrug	XP_027653113.1	94.8	93.4
Gallus gallus	XP_004936086.1	95.5	94.1
Pitangus sulphuratus	KAJ7395145.1	95.5	93.9
Aix galericulata	KAI6069434.1	95.7	94.3
Manacus candei	XP_051646350.1	95.5	94.1
Taeniopygia guttata	XP_002193246.2	95.7	94.3
Corvus kubaryi	XP_041909699.1	95.7	94.1
Hirundo rustica	XP_039920329.1	95.7	94.3
Indicator indicator	XP_054238848.1	95.4	92.4
Pterocles gutturalis	KFV09725.1	95.5	94.1
Gavia stellata	XP_009806622.1	95.5	93.9
Manis pentadactyla	KAI5188327.1	95.9	94.6
Pongo abelii	NP_001127337.1	95.9	94.6
Myotis myotis	XP_036189693.1	95.9	94.3
Jaculus jaculus	XP_045017629.1	95.9	94.3
Rattus norvegicus	NP_001178525.1	95.9	94.3
Microtus ochrogaster	XP_005359400.1	95.9	94.6
Otolemur garnettii	XP_003794646.1	95.9	94.3
Sorex araneus	XP_054994269.1	95.9	94.6
Homo sapiens	AAH37574.1	95.9	94.6

3. Results

3.1. Sequence and phylogenetic analysis of bcUSP46

The coding sequence (CDS) of bcUSP46 has been cloned, which consists of 1119 nucleotides, encoding 372 amino acids. The predicted molecular mass and the predicted theoretical isoelectric point (PI) of bcUSP46 are 43 kDa and 6.23, respectively (calculated by EXPASy Compute PI/Mw). According to the genome information of black carp, the *bcUSP46* gene is located on chromosome 20 (at positions 16461381–16476799) and it contains 9 exons (Fig. 1B). We aligned the amino acid sequences of USP46 proteins from black carp (*Mylopharyngodon piceus*), zebrafish (*Danio rerio*), fathead minnow (*Pimephales promelas*), mice (*Mus musculus*), and human (*Homo sapiens*), and found that bcUSP46 is an evolutionarily conserved molecule that has a ubiquitin carboxy-terminal hydrolase (UCH) domain (Fig. 1A). Phylogenetic analysis showed that the bcUSP46 is most closely related to the *M. amblycephala* USP46 (Fig. 1C). Thus, our results indicate that USP46 is highly conserved in evolution.

3.2. Protein expression and subcellular distribution of bcUSP46

Phylogenetic analysis results have demonstrated that USP46 was highly conserved in vertebrates. Subsequently, we employed homology modeling to compare the protein structures of bcUSP46 and human USP46 (hUSP46) using Swiss-model. The results revealed a substantial similarity between the two proteins (Fig. 2A∼C). Furthermore, we transfected plasmids encoding Flag-bcUSP46 into EPC cells and HEK-293T cells, respectively, and investigated the protein expression of bcUSP46 by western blotting. The results showed that bcUSP46 expressed successfully in both fish and mammalian cells, and its molecular weight was ~43 kDa (Fig. 2D&E). Additionally, we transfected Flag-bcUSP46 plasmids into EPC cells, and employed immunofluorescence assay to study the subcellular distribution of bcUSP46. The findings suggested that bcUSP46 is present in both the cytoplasm and nucleus (Fig. 2F).

3.3. bcUSP46 promotes the RLR/IFN signaling

To examine the impact of bcUSP46 on RLR-IFN signaling axis, the reporter assay was conducted. The results indicate that the expression of bcUSP46 alone activated the transcription of bcIFNa and epcIFN promoters 2.8-fold and 1.5-fold to that of control, respectively (Fig. 3A and B), which suggested the positive role of bcUSP46 in interferon signaling. Since the RLR signaling pathway in fish is essential for IFN production, we further explored the possible role of bcUSP46 in this pathway (Xiao et al., 2023). Specifically, we examined the influence of bcUSP46 on bcRIG-Ib, bcMAVS, bcTBK1, bcIRF7, and bcIRF3 induced transcription of bcIFNa promoter. The results showed that when bcUSP46 was co-expressed with the RLR factor, it enhanced the activation folds of bcIFNa promoter mediated by bcRIG-Ib, bcMAVS, and bcTBK1, with the most significant effect on bcTBK1 (Fig. 3C).

3.4. bcUSP46 interacts with bcTBK1

To further confirm the association between bcUSP46 and bcTBK1, we transfected Flag-bcUSP46 with HA-bcTBK1 into HEK-293T cells and conducted a co-IP analysis. The outcomes revealed the detection of the Flag-bcUSP46 band in the protein that was precipitated from HA-bcTBK1, demonstrating the interaction between bcUSP46 and bcTBK1 (Fig. 4A). In addition, immunofluorescence data revealed the presence of bcUSP46 in both the cytoplasm and nucleus but bcUSP46 is co-localized with bcTBK1 in the cytoplasm (Fig. 4B). These results demonstrate that bcUSP46 interacts with bcTBK1.

3.5. bcUSP46 enhances TBK1-mediated antiviral signaling

Given that bcUSP46 interacted with bcTBK1, we proceeded to investigate the regulatory influence of bcUSP46 on bcTBK1-mediated antiviral signaling. EPC cells were transfected with bcUSP46 and/or bcTBK1, and the mRNA levels of *IFN*, *Mx1*, and *PKR* genes were detected at 24 hpt. The results demonstrated that the expression levels of the above genes in the co-transfected group increased 2.8-, 2.0-, and 1.3-fold, respectively, compared to the group that transfected with bcTBK1 alone (Fig. 5A∼C). Moreover, we investigated the transcript levels of these genes under viral infection. We found that the expression of *IFN*, *Mx1*, and *PKR* genes was also significantly higher in the bcUSP46 and bcTBK1 co-expression group than in cells expressing bcTBK1 alone (Fig. 5D∼F).

Next, we examined whether bcUSP46 could promote TBK1-mediated antiviral activity. We transfected bcUSP46 and/or bcTBK1 in EPC cells and infected with SVCV. The crystalline violet staining results indicated that the cytopathic effect was the lowest among all groups in the cells co-expressing bcUSP46 and bcTBK1 (Fig. 6A). We further examined the viral titers and the transcription level of SVCV encoding genes. The results showed that the viral titers and mRNA levels of SVCV-*G*, -*P*, -*N*, and -*M* in co-expressing bcUSP46 and bcTBK1 group were the lowest (Fig. 6B∼F). Collectively, the data clearly indicate that bcUSP46 notably upregulates bcTBK1-mediated antiviral activity against SVCV.

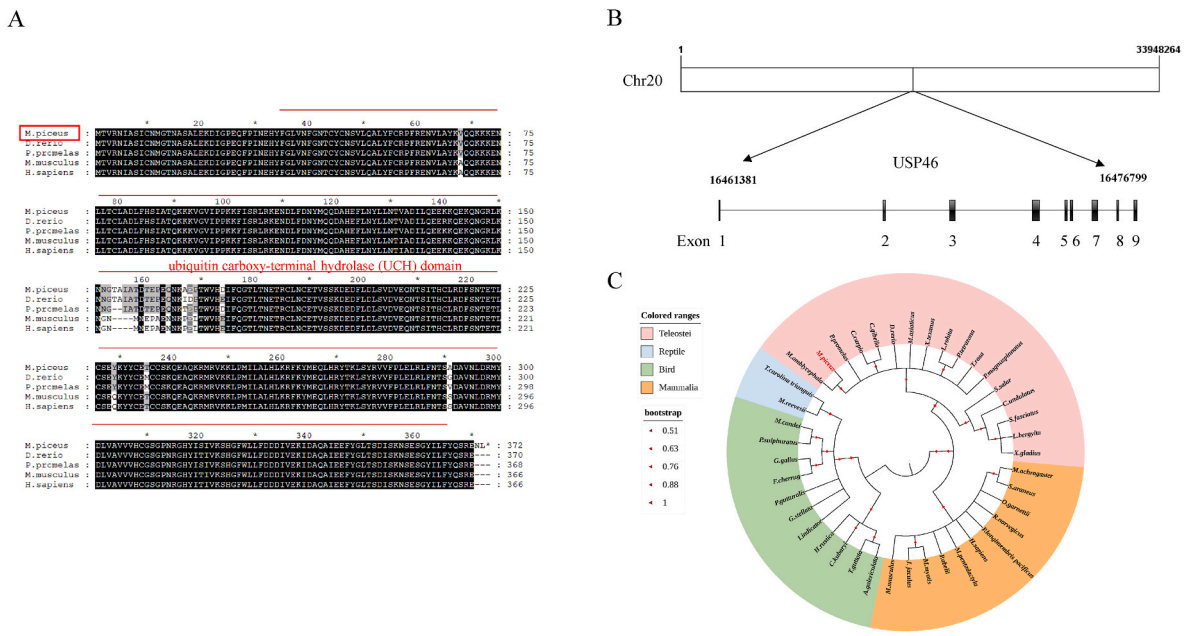

Fig. 1. Sequence and phylogenetic analysis of bcUSP46. (**A**) The amino acid sequences of *H.sapiens*, *M.musculus*, *P.promelas*, *D.rerio*, and *M.piceus* were aligned by MEGA 6.0 and GENEDOC. The UCH domain is indicated by red horizontal lines. (**B**) bcUSP46 genomic information. (**C**) USP46 homologs were aligned and a phylogenetic tree was built using MEGA 6.0 and i-TOL. Genebank accession numbers are given in Table 3. The numbers in Fig. 1C represent bootstraps. (For interpretation of the references to colour in this figure legend, the reader is referred to the Web version of this article.)

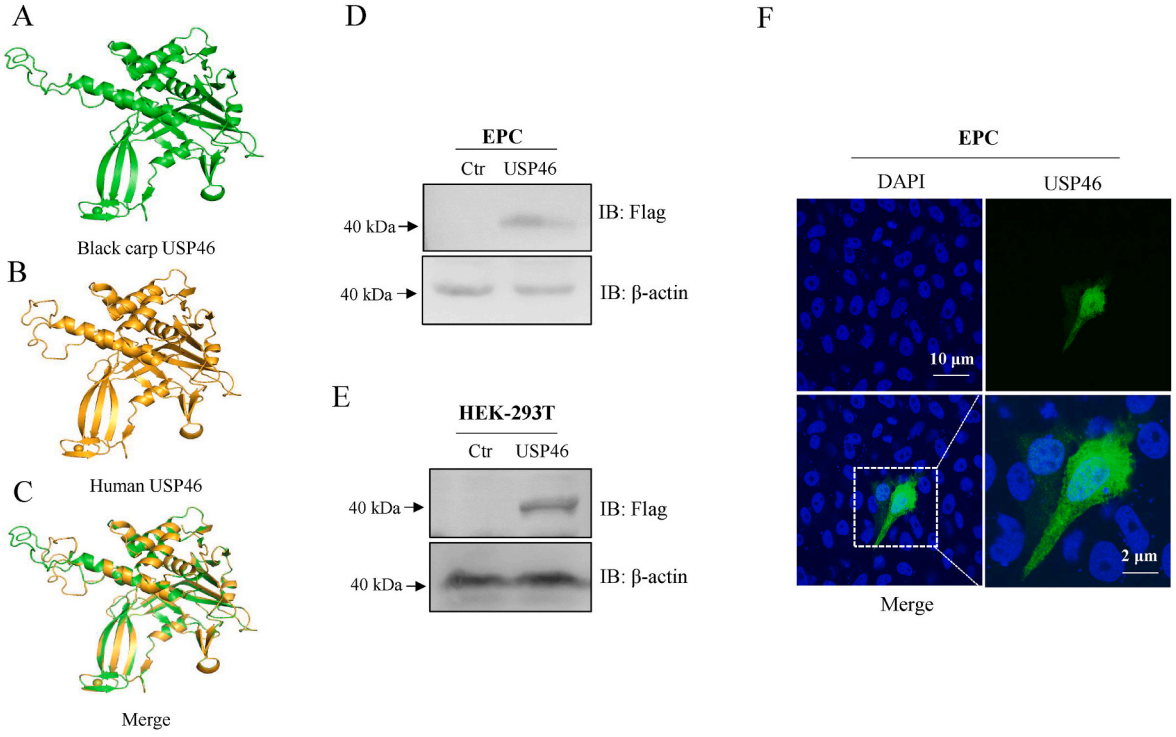

Fig. 2. Protein expression and subcellular distribution of bcUSP46. (**A-C**) Comparison between the three-dimensional structures of human USP46 and bcUSP46. Using SWISS-MODEL and PyMOL to build the homology models. (**D&E**) EPC or HEK-293T cells in 6-well plates were transfected with pcDNA5/FRT/TO-Flag-bcUSP46 (3 μg/well) or the empty vectors pcDNA5/FRT/TO (Ctr). Cells were collected after 48 h for Western-blotting assay. (**F**) EPC cells in 24-well plates were transfected with bcUSP46 (500 ng/well). After 24 h post-transfection, cells were subjected to immunofluorescence assay.

3.6. Knockdown of bcUSP46 reduces MPK cell antiviral ability

To future confirm the antiviral ability of bcUSP46, we performed the knockdown experiment targeting bcUSP46. The IB assay results indicated that shbcUSP46-2# (sh-2) exhibits the highest knockdown efficiency (Fig. 7A). In addition, the mRNA level of *USP46* in MPK cells that were transfected with sh-2 exhibited a decrease of approximately 60% (Fig. 7B). Subsequently, we examined the transcript levels of *IFNa*, *Mx1*, and *Viperin* genes (Fig. 7C~E). We found their mRNA levels decreased significantly after the bcUSP46 knockdown. Furthermore, the

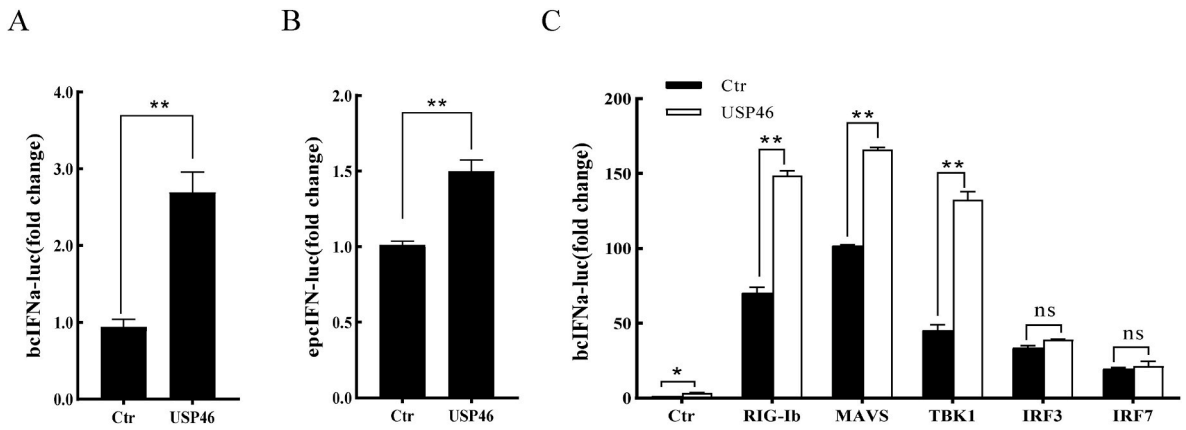

Fig. 3. bcUSP46 promotes bcTBK1-mediated IFN signaling. (**A&B**) EPC cells were co-transfected with bcUSP46 (100 ng/well), Luci-bcIFNa or Luci-epcIFN (250 ng/well), and pRL-TK (50 ng/well) in 24-well plates, respectively. After 24 h, cells were collected for luciferase reporter assay (n = 3). (**C**) EPC cells were transfected with bcUSP46 (100 ng/well) and bcRIG-Ib (bcMAVS, bcTBK1, bcIRF3, or bcIRF7) (100 ng/well), Luci-bcIFNa (250 ng/well), pRL-TK (50 ng/well). The total amount of plasmids for each transfection was balanced with empty vectors, pcDNA5/FRT/TO. After 24 h post-transfection, cells were collected for luciferase reporter assay (n = 3). Asterisk (*) indicates a statistically significant difference (*P < 0.05, **P < 0.01).

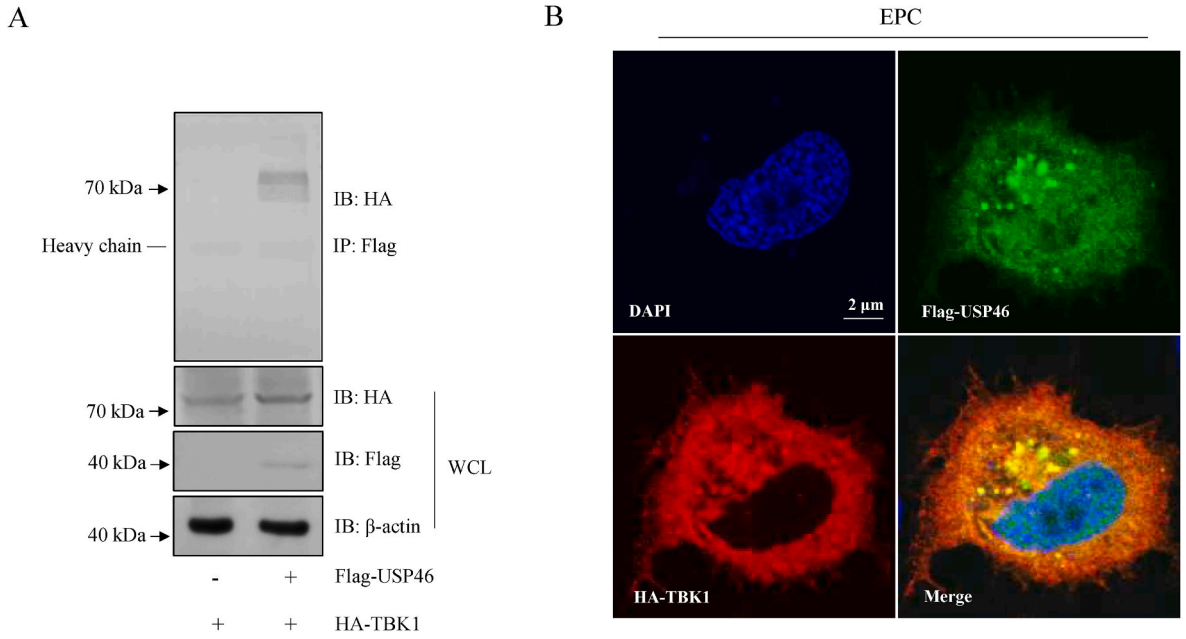

Fig. 4. The interaction between bcUSP46 and bcTBK1. (**A**) HEK-293T cells in 10-cm^2 dishes were co-transfected with 7.5 μg Flag-bcTBK1 and 7.5 μg HA-bcTBK1 (or empty vectors). The cells were harvested for IP assay and subsequential IB assay at 48 hpt. The total amount of plasmids for each transfection was balanced with empty vectors, pcDNA5/FRT/TO. (**B**) EPC cells in 24-well plates were co-transfected with bcUSP46 (250 ng/well) and bcTBK1 (250 ng/well) and the cells were fixed for immunofluorescence microscopy at 24 h post-transfection. The scale bar represented 2 μm.

bcUSP46-knockdown cells were infected with SVCV and the expression of SVCV genes and the viral titer were detected, respectively. The results showed that bcUSP46 knockdown led to an increase in viral replications in MPK cells and an elevated viral titer in the media (Fig. 7F&G). In conclusion, these data further provide evidence of the positive regulatory role of bcUSP46 in host cells against viral infection.

3.7. bcUSP46 removes the K48-linked polyubiquitination of bcTBK1 and promotes its stability

To further elucidate the mechanism of bcUSP46 positive regulating bcTBK1, we transfected EGFP-bcTBK1 plasmids together with different amounts of Flag-bcUSP46 plasmids into HEK-293T cells. As the amounts of bcUSP46 plasmids increased, the protein level of bcTBK1 also gradually increased (Fig. 8A). Considering that bcUSP46 is a deubiquitinating enzyme, we speculate that bcUSP46 may enhance the protein stability of bcTBK1 by removing its polyubiquitination. To confirm this conjecture, we transfected the plasmids encoding Flag-bcTBK1, Myc-bcUSP46, and HA-Ub (or HA-K48O) into HEK-293T cells and detected the ubiquitination level of bcTBK1. As shown in (Fig. 8B), after co-expression with bcUSP46, the wild-type ubiquitination level of bcTBK1 decreased by about 17%, and its K48-linked polyubiquitination level decreased by approximately 21%. Therefore, these data suggest that bcUSP46 removes the K48-linked polyubiquitination of bcTBK1 and promotes its stabilization.

4. Discussion

Virus-triggered IFN signaling is critical for both early innate antiviral responses and late-stage adaptive immunity. TBK1 acts as a key

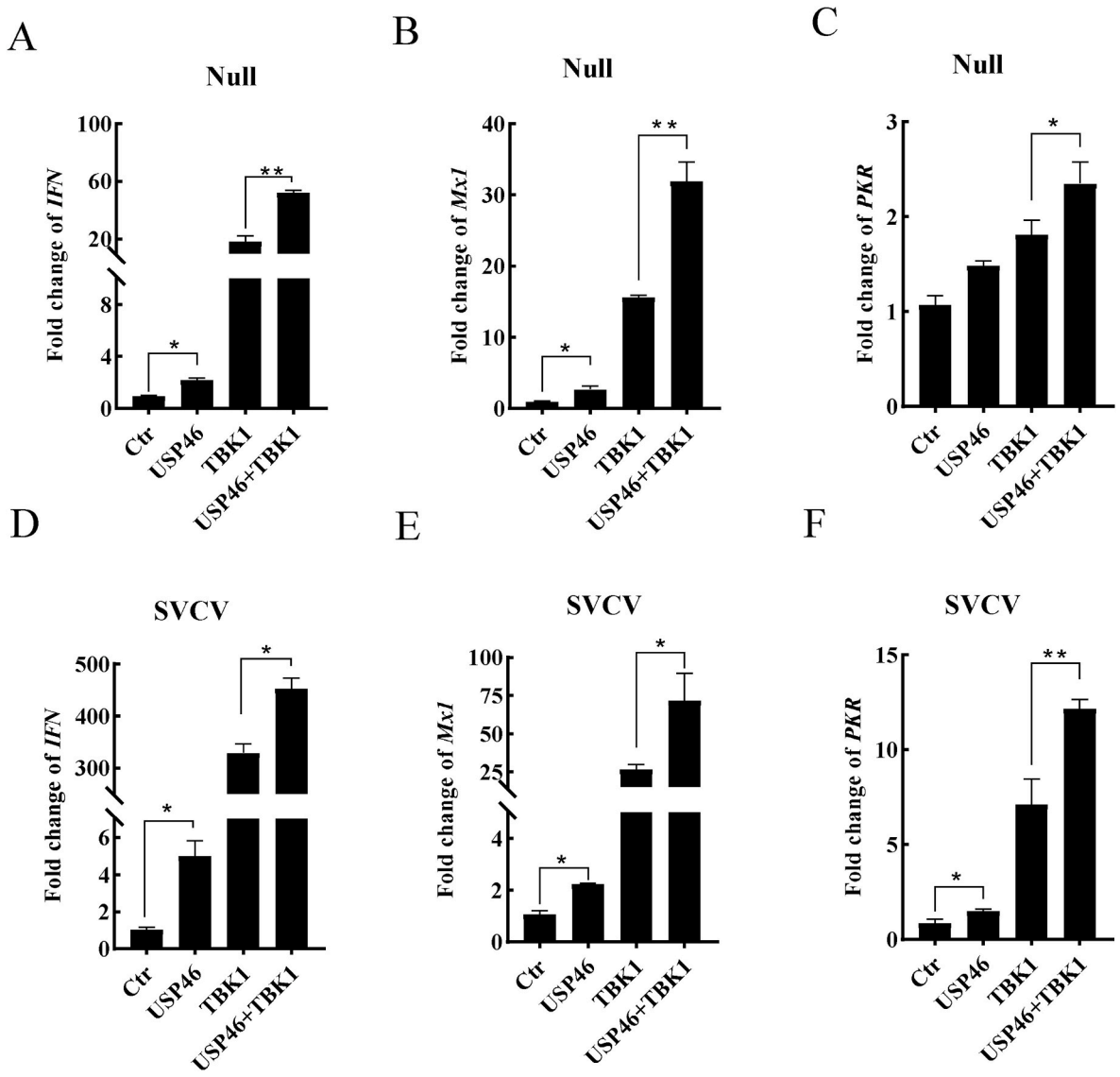

Fig. 5. bcUSP46 induces the mRNA levels of IFN/ISGs in EPC cells. (**A-C**) EPC cells were transfected with bcUSP46 (250 ng/well), bcTBK1 (250 ng/well) or co-transfected with bcUSP46 and bcTBK1, respectively. After 24 hpt, mRNA levels of *IFN*, *PKR*, and *Mx1* were detected. (**D-F**) Transfection was consistent with the above. At 24 hpt, cells were infected with SVCV (MOI = 0.1) for qRT-PCR. Data were analyzed using ANOVA and Tukey test (n = 3).

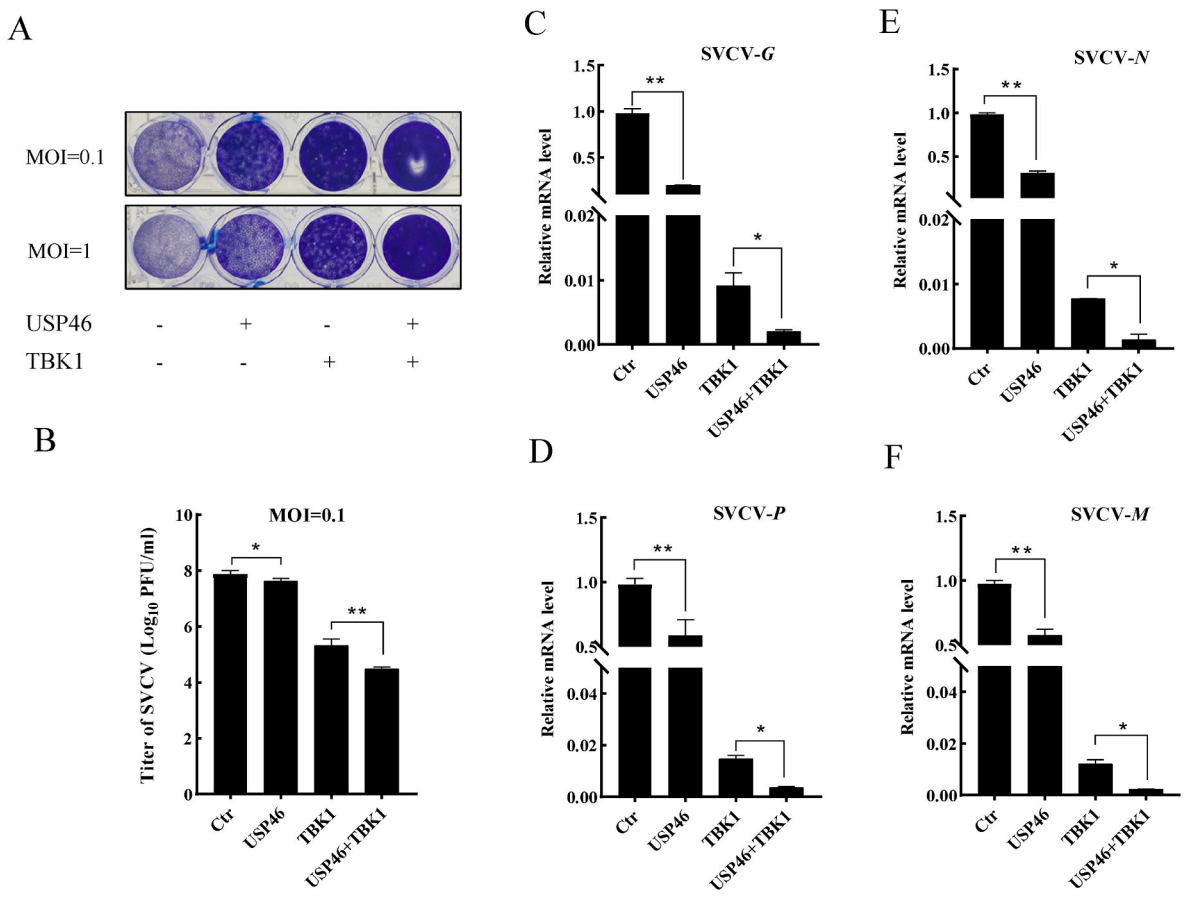

Fig. 6. bcUSP46 positively regulates bcTBK1-mediated antiviral activity. EPC cells in 24-well plates were transfected with bcUSP46 (250 ng/well) and/or bcTBK1 (250 ng/well), respectively. The total amount of plasmids for each transfection was balanced with empty vectors, pcDNA5/FRT/TO. The transfected cells were infected with SVCV (MOI = 0.1 or 1). The monolayer cells were used for crystal violet staining (**A**). The supernatant was collected for virus titer assay (**B**) and cells were harvested for qRT-PCR (**C–F**). Data were analyzed using ANOVA and Tukey test (n = 3). (For interpretation of the references to colour in this figure legend, the reader is referred to the Web version of this article.)

convergence point for the activation in reaction to viruses of DNA and RNA. In mammals, there are many processes involved in controlling TBK1 activity to regulate antiviral signals, such as post-translational modifications (PTMs). For instance, the ubiquitination of TBK1 by E3 ligase RNF128 promotes its stabilization (Song et al., 2016; Zhang et al., 2012). Conversely, TRIP and DTX4-NLRP4 catalyze the K48 ubiquitination of TBK1, leading to its degradation. (Cui et al., 2012). Besides ubiquitination, de-ubiquitination also as a significant role in regulating TBK1 activity. Studies have shown that USP19, USP38, USP2b, and CYLD promote TBK1 degradation through various methods. For example, USP19 accelerates TBK1 degradation in a lysosome-dependent way, but not the proteasome pathway. In addition, USP2b and CYLD achieve attenuation of TBK1 activity by removing the K63-linked ubiquitination of TBK1. Besides, USP38 preferentially degrades K33 ubiquitination from TBK1 at Lys670, and it permits K48 ubiquitination to occur at the same site later through the actions of DTX4 and TRIP to inhibit type I IFN signaling (Friedman et al., 2008; Lin et al., 2016; Zhang et al., 2014). In teleost fish, the activity of TBK1 is also controlled by various factors to sustain homeostasis. For example, SIKE is a suppressor of TBK1, which interacts with TBK1 and inhibits TBK1-mediated antiviral signaling (Li et al., 2019). Additionally, IRF5 interacts with TBK1 to cause cell death to prevent viral multiplication after viral infection (Yang et al., 2019). Besides, zebrafish MARCH8, a membrane-associated RING–CH–type finger family protein, interacts with TBK1 to enable TBK1 degradation, which promotes viral replication by suppressing IFN responses (Zhao et al., 2022). In this investigation, USP46 is a brand-new TBK1 regulator, a deubiquitinating enzyme that positively regulates TBK1/IFN signaling in black carp.

There is evidence that USP46 is associated with a number of human diseases like cancer and neurological disorders. However, its role in innate immunity is rarely studied. In this paper, we explored the function of USP46 in teleost fish. The sequence analysis results showed that USP46 is highly conserved in evolution (Fig. 1A). Besides, the results of the immunofluorescence analysis revealed that bcUSP46 was distributed in both the cytoplasm and the nucleus (Fig. 2F), which is also consistent with the observation of mammalian USP46 (Kiran et al., 2018; Lehoux et al., 2014). Interestingly, we found that overexpression of bcUSP46 enhanced the transcription of Type I IFN promoters and knockdown of bcUSP46 weakened IFNa production (Figs. 3A and 7C). Further analysis revealed that bcUSP46 targeted bcTBK1 and promoted the antiviral activity of bcTKB1. Mechanistically, bcUSP46 promoted the stabilization of bcTBK1 by eliminating its K48-linked ubiquitination. This is consistent with the deubiquitination mechanism of human USP46. For example, in human esophageal squamous cell carcinoma, USP46 stabilizes the ENO1 protein, thereby promoting tumor metastasis. In hepatocellular carcinoma, USP46 enhances MST1 kinase activity, and inhibits tumor growth and metastasis (Qiu et al., 2021; Tian et al., 2020). Furthermore, the deubiquitinating activity of USP46 in mice is associated with its lysine 92 residue (Zhang et al., 2011). Since USP46 is a highly conserved gene, the residue 92 of bcUSP46 is also a lysine, which provides a clue for us to further explore the deubiquitinating activity site of bcUSP46.

USP46, as a deubiquitinating enzyme with numerous substrates, can not only modify host proteins but also interact with viral proteins. For

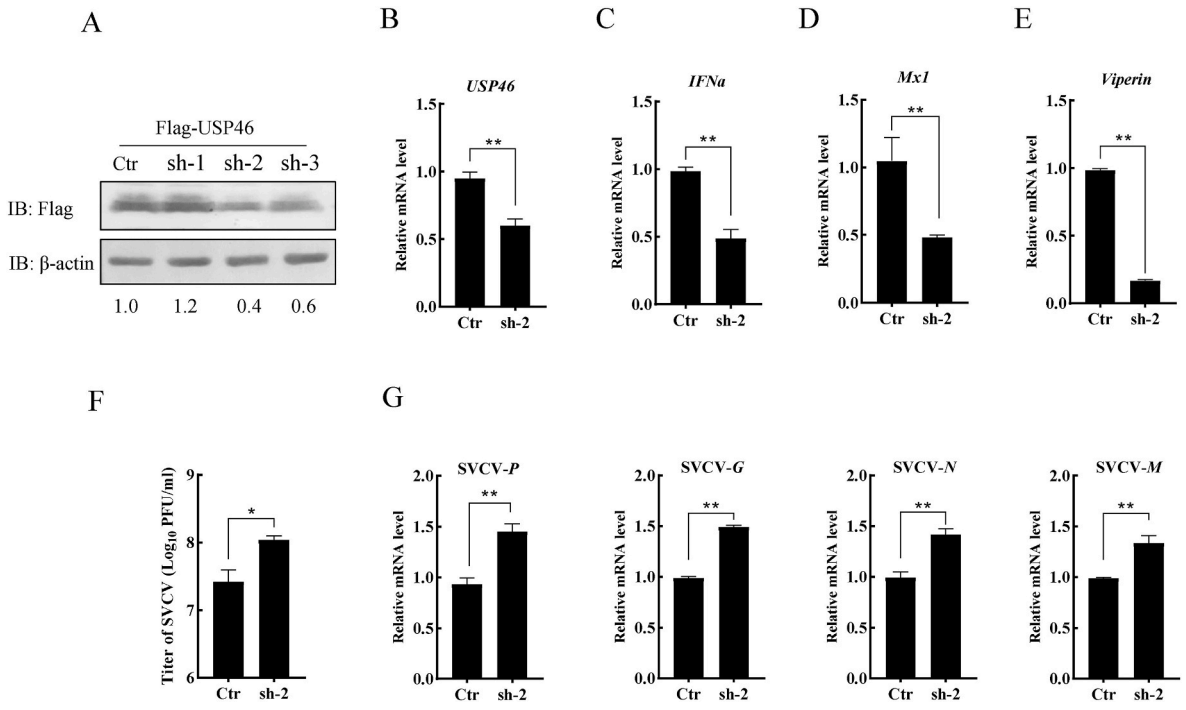

Fig. 7. Knock-down of bcUSP46 suppresses the host antiviral signaling. (A) HEK-293T cells in 6-well plates were co-transfected with Flag-bcUSP46 (1.5 μg/well) and pLKO.1-sh-bcUSP46-1/2/3 (or pLKO.1-sh-scramble, 1.5 μg/well, as control). Cells were lysed at 24 hpt for immunoblotting. (**B-E**) MPK cells were transfected with pLKO.1-sh-bcUSP46-2 or pLKO.1-sh-scramble and the mRNA levels of bcUSP46, IFN, and ISGs were detected by qRT-PCR analysis at 24 hpt. (**F&G**) MPK cells were transfected with pLKO.1-sh-bcUSP46-2 or pLKO.1-sh-scramble and infected with SVCV (MOI = 0.1) 24 h after transfection. The supernatants were collected at 24h post-infection for viral titer detection **(F)**. The cells were collected and the mRNA levels of SVCV-encoding genes were detected by qRT-PCR **(G)**.

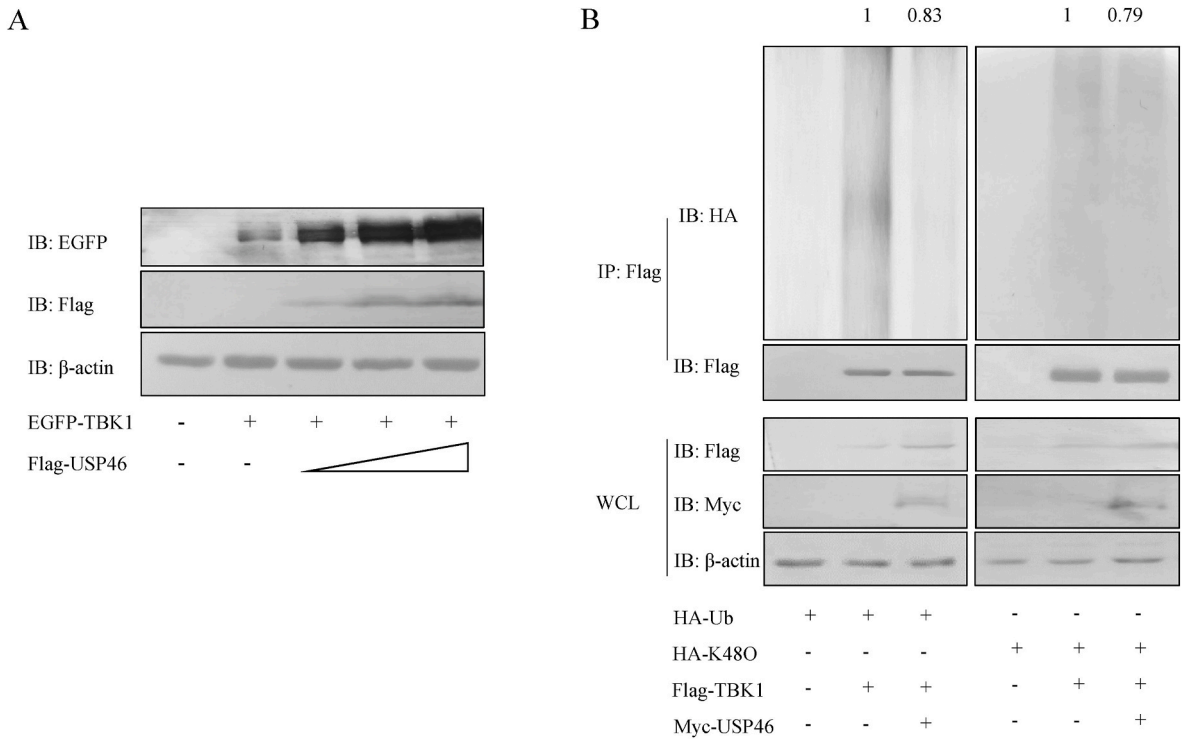

Fig. 8. bcUSP46 removes K48-linked polyubiquitination of bcTBK1 and promotes its stabilization. (**A**) HEK-293T cells were co-transfected with EGFP-bcTBK1 (500 ng/well) and Flag-bcUSP46 (0.5, 2, or 3 μg/well). The total amount of plasmids for each transfection was balanced with empty vectors. Then the cells were collected for IB assay at 48 hpt. (**B**) HEK-293T cells co-transfected with HA-Ub (or HA-Ub-K48O) (6μg/well), Myc-bcUSP46 (6μg/well) and/or Flag-bcTBK1(3μg/well) were collected for co-IP assay and IB assay at 48 hpt. The relative ubiquitination levels were calculated for each lane using ImageJ software (normalized to the expression level of Flag-bcTBK1). The total amount of plasmids for each transfection was balanced with empty vectors, pcDNA5/FRT/TO.

instance, the Epstein-Barr virus (EBV) is related to the pathogenesis of several malignant tumors. USP46 associates with EBV nuclear proteins EBNA3A/3B/3C to promote EBV-induced growth transformation. In addition, under high-risk human papillomavirus (HPV) infection, USP46 binds to the E6 protein of HPV and deubiquitinates Cdt2/DTL, thereby permitting cancer cell proliferation and tumor growth (Kiran et al., 2018; Lehoux et al., 2014; Ohashi et al., 2015). Among fish viruses, SVCV causes serious death of fish. It encodes five essential structural proteins sequentially: N, P, M, G, and L (Hoffmann et al., 2002; Teng et al., 2007). Several studies have reported that the activity of SVCV-encoded proteins is also affected by deubiquitination modifications during SVCV infection. For instance, zebrafish ceramide kinase-like (CERKL) is a vital part in anti-viral response because it can eliminate SVCV P proteins through obstructing K63-linked ubiquitination (Chen et al., 2022). In addition, zebrafish mitogen-activated protein kinase 7 (MAP2K7) attenuates K63-mediated polyubiquitination of SVCV-P, causing its degradation (Zhang et al., 2023). Therefore, exploring the relationship between USP46 and viral proteins, such as whether USP46 modifies SVCV-encoded proteins by deubiquitination to inhibit the function of viral proteins, is worth investigating in our subsequent work.

In summary, this study found that bcUSP46 is a positive regulator of bcTBK1. Mechanistically, it binds to bcTBK1 and enhances its stability by eliminating the K48 polyubiquitination of bcTBK1. Thus, these results suggest a significant function of USP46 in regulating TBK1/IFN signaling and provide new insights for a deeper comprehension of the regulatory mechanisms of the IFN signaling pathway in vertebrates.

CRediT authorship contribution statement

Juanjuan Shu: Validation, Methodology. **Can Yang:** Validation, Methodology. **Yujia Miao:** Validation. **Jinyi Li:** Writing – review & editing, Formal analysis, Conceptualization. **Tianle Zheng:** Zewen Yi: Investigation. **Jun Xiao:** Validation, Methodology. **Weiguang Kong:** Validation. **Zhen Xu:** Writing – review & editing, Supervision, Conceptualization. **Hao Feng:** Validation, Investigation.

Declaration of competing interest

The authors declare that the research was conducted in the absence of any commercial or financial relationships that could be construed as a potential conflict of interest.

Data availability

Data will be made available on request.

Acknowledgements

This work was supported by the National Natural Science Foundation of China (31920103016, U21A20268, U22A20535, 32002383), Hunan Provincial Science and Technology Department (2023JJ40435), the Modern Agricultural Industry Program of Hunan Province, the Research and Development Platform of Fish Disease and Vaccine for Postgraduates in Hunan Province, Hunan Provincial Education Department (23B0070), Hunan province college students research learning and innovative experiment project (S202310542057, S202310542102).

References

Cao, X., 2016. Self-regulation and cross-regulation of pattern-recognition receptor signalling in health and disease. Nat. Rev. Immunol. 16 (1), 35–50. http://10.1038/nri.2015.8.

Chen, D.D., Lu, L.F., Xiong, F., Wang, X.L., Jiang, J.Y., Zhang, C., Li, Z.C., Han, K.J., Li, S., 2022. Zebrafish CERKL enhances host TBK1 stability and simultaneously degrades viral protein via ubiquitination modulation. J. Immunol. 208 (9), 2196–2206. http://10.4049/jimmunol.2101007.

Cui, J., Li, Y., Zhu, L., Liu, D., Songyang, Z., Wang, H.Y., Wang, R.F., 2012. NLRP4 negatively regulates type I interferon signaling by targeting the kinase TBK1 for degradation via the ubiquitin ligase DTX4. Nat. Immunol. 13 (4), 387–395. http://10.1038/ni.2239.

Fitzgerald, K.A., McWhirter, S.M., Faia, K.L., Rowe, D.C., Latz, E., Golenbock, D.T., Coyle, A.J., Liao, S.M., Maniatis, T., 2003. IKKepsilon and TBK1 are essential components of the IRF3 signaling pathway. Nat. Immunol. 4 (5), 491–496. http://10.1038/ni921.

Friedman, C.S., O'Donnell, M.A., Legarda-Addison, D., Ng, A., Cárdenas, W.B., Yount, J. S., Moran, T.M., Basler, C.F., Komuro, A., Horvath, C.M., Xavier, R., Ting, A.T., 2008. The tumour suppressor CYLD is a negative regulator of RIG-I-mediated antiviral response. EMBO Rep. 9 (9), 930–936. http://10.1038/embor.2008.136.

Hodul, M., Dahlberg, C.L., Juo, P., 2017. Function of the deubiquitinating enzyme USP46 in the nervous system and its regulation by WD40-repeat proteins. Front. Synaptic Neurosci. 9, 16. http://10.3389/fnsyn.2017.00016.

Hoffmann, B., Schütze, H., Mettenleiter, T.C., 2002. Determination of the complete genomic sequence and analysis of the gene products of the virus of Spring Viremia of Carp, a fish rhabdovirus. Virus Res. 84 (1–2), 89–100. http://10.1016/s0168-1702(01)00441-5.

Joo, H.Y., Jones, A., Yang, C., Zhai, L., Smith, ADt, Zhang, Z., Chandrasekharan, M.B., Sun, Z.W., Renfrow, M.B., Wang, Y., Chang, C., Wang, H., 2011. Regulation of histone H2A and H2B deubiquitination and Xenopus development by USP12 and USP46. J. Biol. Chem. 286 (9), 7190–7201. http://10.1074/jbc.M110.158311.

Kiran, S., Dar, A., Singh, S.K., Lee, K.Y., Dutta, A., 2018. The deubiquitinase USP46 is essential for proliferation and tumor growth of HPV-transformed cancers. Mol. Cell 72 (5), 823–835.e825. http://10.1016/j.molcel.2018.09.019.

Komander, D., Clague, M.J., Urbé, S., 2009. Breaking the chains: structure and function of the deubiquitinases. Nat. Rev. Mol. Cell Biol. 10 (8), 550–563. http://10.1038/nrm2731.

Lehoux, M., Gagnon, D., Archambault, J., 2014. E1-mediated recruitment of a UAF1-USP deubiquitinase complex facilitates human papillomavirus DNA replication. J. Virol. 88 (15), 8545–8555. http://10.1128/jvi.00379-14.

Li, J., Yan, C., Liu, J., Yan, J., Feng, H., 2019. SIKE of black carp is a substrate of TBK1 and suppresses TBK1-mediated antiviral signaling. Dev. Comp. Immunol. 90, 157–164. http://10.1016/j.dci.2018.09.016.

Li, S., Wang, L., Berman, M., Kong, Y.Y., Dorf, M.E., 2011. Mapping a dynamic innate immunity protein interaction network regulating type I interferon production. Immunity 35 (3), 426–440. http://10.1016/j.immuni.2011.06.014.

Lin, M., Zhao, Z., Yang, Z., Meng, Q., Tan, P., Xie, W., Qin, Y., Wang, R.F., Cui, J., 2016. USP38 inhibits type I interferon signaling by editing TBK1 ubiquitination through NLRP4 signalosome. Mol. Cell 64 (2), 267–281. http://10.1016/j.molcel.2016.08.029.

Ohashi, M., Holthaus, A.M., Calderwood, M.A., Lai, C.Y., Krastins, B., Sarracino, D., Johannsen, E., 2015. The EBNA3 family of Epstein-Barr virus nuclear proteins associates with the USP46/USP12 deubiquitination complexes to regulate lymphoblastoid cell line growth. PLoS Pathog. 11 (4), e1004822. http://10.1371/journal.ppat.1004822.

Qiu, Y., Huang, D., Sheng, Y., Huang, J., Li, N., Zhang, S., Hong, Z., Yin, X., Yan, J., 2021. Deubiquitinating enzyme USP46 suppresses the progression of hepatocellular carcinoma by stabilizing MST1. Exp. Cell Res. 405 (1), 112646. http://10.1016/j.yexcr.2021.112646.

Runde, A.P., Mack, R., S, J.P., Zhang, J., 2022. The role of TBK1 in cancer pathogenesis and anticancer immunity. J. Exp. Clin. Cancer Res. 41 (1), 135. http://10.1186/s13046-022-02352-y.

Song, G., Liu, B., Li, Z., Wu, H., Wang, P., Zhao, K., Jiang, G., Zhang, L., Gao, C., 2016. E3 ubiquitin ligase RNF128 promotes innate antiviral immunity through K63-linked ubiquitination of TBK1. Nat. Immunol. 17 (12), 1342–1351. http://10.1038/ni.3588.

Teng, Y., Liu, H., Lv, J.Q., Fan, W.H., Zhang, Q.Y., Qin, Q.W., 2007. Characterization of complete genome sequence of the spring viremia of carp virus isolated from common carp (Cyprinus carpio) in China. Arch. Virol. 152 (8), 1457–1465. http://10.1007/s00705-007-0971-8.

Tian, M., Zhu, R., Ding, F., Liu, Z., 2020. Ubiquitin-specific peptidase 46 promotes tumor metastasis through stabilizing ENO1 in human esophageal squamous cell carcinoma. Exp. Cell Res. 395 (1), 112188. http://10.1016/j.yexcr.2020.112188.

Wang, C., Chen, T., Zhang, J., Yang, M., Li, N., Xu, X., Cao, X., 2009. The E3 ubiquitin ligase Nrdp1 'preferentially' promotes TLR-mediated production of type I interferon. Nat. Immunol. 10 (7), 744–752. http://10.1038/ni.1742.

Xiao, J., Zhong, H., Feng, H., 2023. Post-translational modifications and regulations of RLR signaling molecules in cytokines-mediated response in fish. Dev. Comp. Immunol. 141, 104631. http://10.1016/j.dci.2023.104631.

Yang, C., Liu, L., Liu, J., Ye, Z., Wu, H., Feng, P., Feng, H., 2019. Black carp IRF5 interacts with TBK1 to trigger cell death following viral infection. Dev. Comp. Immunol. 100, 103426. http://10.1016/j.dci.2019.103426.

Yang, Q., Yan, D., Zou, C., Xue, Q., Lin, S., Huang, Q., Li, X., Tang, D., Chen, X., Liu, J., 2022. The deubiquitinating enzyme STAMBP is a newly discovered driver of triple-negative breast cancer progression that maintains RAI14 protein stability. Exp. Mol. Med. 54 (11), 2047–2059. http://10.1038/s12276-022-00890-1.

Yin, J., Schoeffler, A.J., Wickliffe, K., Newton, K., Starovasnik, M.A., Dueber, E.C., Harris, S.F., 2015. Structural insights into WD-repeat 48 activation of ubiquitin-specific protease 46. Structure 23 (11), 2043–2054. http://10.1016/j.str.2015.08.010.

Zhang, C., Lu, L.F., Li, Z.C., Han, K.J., Wang, X.L., Chen, D.D., Xiong, F., Li, X.Y., Zhou, L., Ge, F., Li, S., 2023. Zebrafish MAP2K7 simultaneously enhances host IRF7 stability and degrades spring viremia of carp virus P protein via ubiquitination pathway. J. Virol., e0053223. http://10.1128/jvi.00532-23.

Zhang, L., Zhao, X., Zhang, M., Zhao, W., Gao, C., 2014. Ubiquitin-specific protease 2b negatively regulates IFN-β production and antiviral activity by targeting TANK-binding kinase 1. J. Immunol. 193 (5), 2230–2237. http://10.4049/jimmunol.1302634.

Zhang, M., Wang, L., Zhao, X., Zhao, K., Meng, H., Zhao, W., Gao, C., 2012. TRAF-interacting protein (TRIP) negatively regulates IFN-β production and antiviral response by promoting proteasomal degradation of TANK-binding kinase 1. J. Exp. Med. 209 (10), 1703–1711. http://10.1084/jem.20120024.

Zhang, W., Tian, Q.B., Li, Q.K., Wang, J.M., Wang, C.N., Liu, T., Liu, D.W., Wang, M.W., 2011. Lysine 92 amino acid residue of USP46, a gene associated with 'behavioral despair' in mice, influences the deubiquitinating enzyme activity. PLoS One 6 (10), e26297. http://10.1371/journal.pone.0026297.

Zhao, X., Dan, C., Gong, X.Y., Li, Y.L., Qu, Z.L., Sun, H.Y., An, L.L., Guo, W.H., Gui, J.F., Zhang, Y.B., 2022. Zebrafish MARCH8 downregulates fish IFN response by targeting MITA and TBK1 for protein degradation. Dev. Comp. Immunol. 135, 104485. http://10.1016/j.dci.2022.104485.